Biosensors and Bioelectronics 140 (2019) 111343

Contents lists available at ScienceDirect

Biosensors and Bioelectronics

journal homepage: www.elsevier.com/locate/bios

Flexible electrochemical glucose biosensor based on GOx/gold/MoS_2/gold nanofilm on the polymer electrode

Jinho Yoon[a], Sang Nam Lee[b], Min Kyu Shin[a], Hyun-Woong Kim[a], Hye Kyu Choi[a], Taek Lee[c], Jeong-Woo Choi[a,*]

[a] Department of Chemical & Biomolecular Engineering, Sogang University, 35 Baekbeom-Ro, Mapo-Gu, Seoul, 04107, Republic of Korea
[b] Scien US Inc., 1107 Teilhard Hall, 35 Baekbeom-Ro, Mapo-Gu, Seoul, 04107, Republic of Korea
[c] Department of Chemical Engineering, Kwangwoon University, Wolgye-dong, Nowon-gu, Seoul, 01899, Republic of Korea

ARTICLE INFO

Keywords:
Biosensor
Sputter deposition of gold
Spin coating
MoS_2 nanoparticle
Glucose
Flexibility

ABSTRACT

The need for flexible biosensors has increased because of their potential applications for point-of-care diagnosis and wearable biosensors. However, flexible biosensors have low sensitivity due to the flexibility of the electrode, and their fabrication involves complex processes. To overcome these limitations, a flexible electrochemical enzyme biosensor was developed in this study by immobilizing an enzyme on the flexible polymer electrode modified with a gold/MoS_2/gold nanofilm. The fabrication process involved sputter deposition of gold, spin coating of MoS_2, and sputter deposition of gold on the flexible polymer electrode (commercially available Kapton® polyimide film). The flexible glucose biosensor was made by immobilization of glucose oxidase on a flexible electrode by using a chemical linker. The detection limit for glucose was estimated to be 10 nM, which indicates more sensitivity as compared with a previously reported flexible glucose sensor. This sensitivity is due to the facilitation of electron transfer by MoS_2. The flexure extension of this biosensor was estimated at 3.48 mm, which is much higher than that of the rigid sensor using a gold-coated silicon electrode (0.09 mm), according to measurements with a micro-fatigue tester. The proposed flexible biosensor composed of the enzyme/gold/MoS_2/gold nanofilm on the polymer electrode can be used as a flexible sensing platform for developing wearable biosensing systems because of its high sensitivity, high flexibility, and simple fabrication process.

1. Introduction

Because of the fast development of wearable and wireless electronic devices, there is much interest in the development of flexible electrodes (Kang et al., 2015). Flexible polymers have potential applications in point-of-care diagnosis systems (> Wang et al., 2016a,b) and wearable biosensing systems. Bendable polymers such as poly(ethylene terephthalate) are widely used to confer flexibility to the electrode (Zhao et al., 2018). Flexible polymers, including Kapton® polyimide film, are cheap and easy to acquire. A complex fabrication processes such as photolithography or an intricate surface modification process has been used to develop flexible conductive electrodes for biosensor applications (Wang et al., 2016a,b; Yang et al., 2017). The flexible biosensors have low sensitivity due to the flexibility of the nonconductive polymer electrode (Wang et al., 2016a,b). Simple surface modification techniques and versatile metal nanoparticles can overcome these limitations. To achieve flexibility with high sensitivity and a simple fabrication process, sputter deposition can be introduced to easily modify the surface of the flexible polymer. Metallic nanomaterials can be used as electron-transfer facilitators to impart conductivity to the nonconductive polymer.

To increase the signal and the electron transfer rate, various materials have been used to develop biosensors (Zhu, 2017). Carbon nanotubes and graphene may be the most widely known nanomaterials used in applications such as induction of stem cell differentiation and electrochemical signal increment (Fenzl et al., 2016; Gardin et al., 2016). Recently, metal dichalcogenides (TMDs) such as molybdenum disulfide (MoS_2) have been used for biological applications. TMDs have excellent conductivity and can be used in biosensors, bioelectronics, and electrochemical actuators (Wang et al., 2015; Wang et al, 2013; Acerce et al., 2017). Our group also used MoS_2 to develop a highly sensitive biosensor (Yoon et al., 2017a,b). Simultaneous use of MoS_2 and flexible polymeric materials as the electrode creates a synergetic effect for the fabrication of a flexible biosensor platform (Shafiee et al., 2015). Furthermore, simultaneous sputter deposition and spin coating (Reimhult et al., 2008; Tyona, 2013) of MoS_2 can lead to the formation of flexible

* Corresponding author.
E-mail address: jwchoi@sogang.ac.kr (J.-W. Choi).

https://doi.org/10.1016/j.bios.2019.111343
Received 5 March 2019; Received in revised form 13 May 2019; Accepted 20 May 2019
Available online 25 May 2019
0956-5663/

conductive electrodes. This simple fabrication process for flexible biosensor fabrication has not been reported yet.

In the development of the biosensor, glucose is an important target molecule because excessively high concentration of glucose in the blood can cause diabetes mellitus (Torimoto et al., 2013; Abikshyeet et al., 2012). Diabetes mellitus can cause death and disability in humans (Manson et al., 1991; Alberti and Zimmet, 1998; Tuomilehto et al., 2001; Ray et al., 2009). Enzyme-based biosensors can detect glucose accurately because of their rapid electrochemical responses (Rogers, 2006; Baghayeri et al., 2016; Ahammad et al., 2016; Zhao et al., 2017). Glucose oxidase (GOx) is a protein that has glucose-sensing abilities (Schuhmann et al., 1991; Wilson and Turner, 1992; Wu et al., 2015). GOx can oxidize glucose to gluconic acid and hydrogen peroxide (Ferri et al., 2011; Yoo and Lee, 2010; Chaichi and Ehsani, 2016). However, enzyme-based biosensors have some limitations such as low electrochemical signal due to the low electron-transfer rate (Min et al., 2010). By introduction of MoS_2, the electrochemical signal from the enzyme can be increased and it can be easily detected.

In this study, GOx/gold/MoS_2/gold nanofilm on a polymer electrode was fabricated for the first time to develop a glucose-detecting biosensor with high sensitivity, selectivity, and flexibility. The nanofilm on the polymer electrode was fabricated simply by sputter deposition of gold and spin coating of MoS_2. This gold/MoS_2/gold nanofilm on the polymer electrode increased the electrochemical signal and made the biosensor flexible. The glucose-sensing biomolecule, GOx, was immobilized on the gold/MoS_2/gold nanofilm on the polymer electrode through a chemical linker (Fig. 1). Fabrication of the nanofilm on the polymer electrode was verified by scanning electron microscopy (SEM) and energy-dispersive X-ray spectroscopy (EDS) with EDS mapping. Surface morphology was investigated by atomic force microscopy (AFM). Cyclic voltammetry (CV) was used to confirm the immobilization of GOx and to investigate the electrochemical properties of the fabricated biosensors (Lee et al., 2019a). To estimate the glucose-sensing property, amperometric I–T measurements were done by addition of glucose. The flexibility of the fabricated biosensors was investigated by using a micro-fatigue tester (E3000LT, Instron, UK).

2. Experimental details

2.1. Materials

N,*N*-Dimethyl formaldehyde (DMF) used for dissolving MoS_2 nanoparticles (NPs) and acetone used for the polymer electrode washing were purchased from Daejung Chemical (Korea). GOx from *Aspergillus niger* and myoglobin (Mb) were acquired from Sigma-Aldrich (USA). Phosphate-buffered saline (PBS) solution was prepared using PBS powder obtained from Sigma-Aldrich (USA). D-Glucose was acquired from Junsei (Japan).

The chemical linker 6-mercaptohexanoic acid (6-MHA) was purchased from Sigma-Aldrich, and hydrogen peroxide and sulfuric acid for the piranha solution were purchased from Daejung Chemical (Korea). Deionized (DI) water was prepared by using a Milli-Q system (Millipore, USA). Sodium molybdate and hydrazine hydrate from Sigma-Aldrich were used for MoS_2 NP synthesis. A gold-coated silicon electrode composed of gold (50 nm), Cr (2 nm), and SiO_2 for the control-electrode preparation was fabricated by the National Nanofab Center (Korea). L-Ascorbic acid (AA) and uric acid (UA) were purchased from Sigma-Aldrich. The polymer (Kapton® polyimide film) electrode (Kapton, PV9101, 50 μm) was obtained from Dupont (USA). A gold sputtering machine (108 Auto sputter coater, Cressington Scientific Instruments, UK) was used. A spin coater (JS301) from Jaesung Engineering (Korea) was used for MoS_2 NP spin coating. Human serum was purchased from Sigma-Aldrich to detect glucose in an actual sample.

2.2. Fabrication of the gold/MoS_2/gold nanofilm on the polymer electrode

MoS_2 NPs were synthesized through a synthetic process previously used by our group (Yoon et al., 2017a,b; Yoon et al., 2017a,b; Mohammadniaei et al., 2018). The synthesized MoS_2 NPs were dissolved in DMF and sonicated for dispersion. To prepare the gold/MoS_2/gold nanofilm, the polymer electrode was sonicated for 30 min in acetone to remove dust from the surface of the electrode. After cleaning with acetone, the polymer electrode was washed with ethanol and DI water and dried fully with N_2 gas. Gold was uniformly deposited on the surface of the cleaned polymer electrode with a gold-sputtering machine. The synthesized MoS_2 NPs (100 μL of 10 mg/mL) were dissolved in DMF and applied dropwise on the gold-deposited polymer electrode. The electrode was spin-coated for 30 s at 3000 rpm to form the MoS_2 layer. Gold was sputtered once more on the MoS_2 layer using the gold-sputtering machine to form the gold/MoS_2/gold nanofilm on the polymer electrode. The gold/MoS_2/gold nanofilm was characterized by SEM, EDS, and AFM.

2.3. Immobilization of GOx on the gold/MoS_2/gold nanofilm

The fabricated gold/MoS_2/gold nanofilm on the polymer electrode was washed with ethanol and DI water to make the surface clean for immobilization of the GOx. The GOx was dissolved in PBS at 0.2 mg/mL concentration. The chemical linker, 6-MHA, was prepared in ethanol and immobilized on the surface of the nanofilm for 3 h at 4 °C through the gold–thiol interaction. Twenty microliters of dissolved GOx in PBS was then applied dropwise to the nanofilm for 3 h at 4 °C. The flexible biosensor was fabricated by immobilization of GOx on the electrode

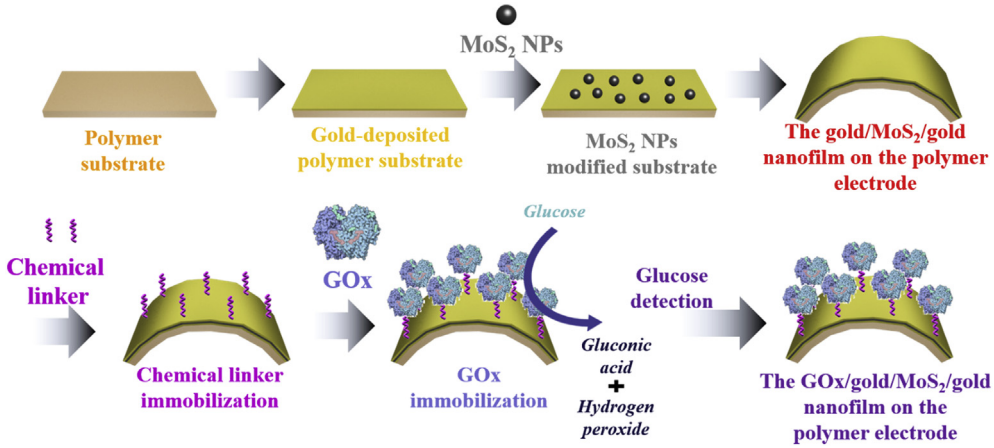

Fig. 1. Schematic diagram of the fabrication of a flexible electrochemical glucose biosensor composed of a GOx/gold/MoS_2/gold nanofilm on the polymer electrode.

through electrostatic interaction between 6-MHA and the GOx. The other electrodes were prepared to compare with this biosensor. To investigate the increments in the electrochemical signal, GOx was immobilized on the polymer electrode with deposited gold only, the conventional gold-coated silicon electrode, and the gold/MoS_2/gold nanofilm on the conventional gold-coated silicon electrode for comparison. To investigate the flexibility of the gold/MoS_2/gold nanofilm on the polymer electrode, gold-coated gold (50 nm)/Cr (2 nm)/SiO_2 electrode was used as the control. To clean this gold electrode, a piranha solution was prepared using H_2O_2 and H_2SO_4 at 2:8 ratio. After treatment with the piranha solution for 3 min, the gold electrode was washed using ethanol and DI water sequentially, and then fully dried with N_2 gas. During GOx immobilization on the nanofilm, GOx was immobilized on the gold-coated silicon electrode. Immobilization of GOx on the nanofilm was verified by CV through the redox signal derived from GOx.

2.4. Surface investigation of the biosensor

The surface morphology of the GOx/gold/MoS_2/gold nanofilm on the polymer electrode was investigated by SEM (JSM-7100F, JEOL, USA). Platinum was deposited on the surface of the prepared electrode to study its morphology. The surface characteristics of the bare polymer electrode and the gold-coated polymer electrode were studied. During the SEM investigation, EDS analysis was done to confirm the elemental components located on the electrode. After the SEM image of the surface was acquired, the EDS mapping technique was used to verify the components on the surface of the electrode at the SEM location. AFM was also conducted to further study the surface (Lee et al., 2019b). To verify the layer formation, the surface characteristics of the bare polymer electrode, gold-coated polymer electrode, and gold/MoS_2/gold nanofilm on the polymer electrode were investigated and compared.

2.5. Investigation of electrochemical properties and glucose-sensing performance of the fabricated biosensor

Electrochemical investigation of the prepared GOx/gold/MoS_2/gold nanofilm was performed through an electrochemical technique using a CHI-660A machine (CH Instruments, Inc., USA) (Lee et al., 2010). Electrochemical investigation was done using a conventional three-electrode system with a PBS solution used as the electrolyte. The prepared GOx/gold/MoS_2/gold nanofilm on the polymer electrode was used as the working electrode. The silver/silver chloride (Ag/AgCl) double-junction reference electrode was used as the reference electrode, and the platinum (Pt) wire electrode was used as the counter electrode. The parameters for CV measurement were as follows: quiet time of 2 s, sampling interval of 1 mV/s, scan rate of 50 mV/s, and a sensitivity of 5×10^{-4} (A/V). The applied voltage range was 600 mV to −800 mV. To confirm the electrochemical signal increment, the GOx/gold-coated silicon electrode, the GOx/gold-coated polymer electrode, and the GOx/gold/MoS_2/gold nanofilm on the conventional gold-coated silicon electrode were fabricated for comparison. After CV measurement, the glucose-sensing property of the prepared GOx/gold/MoS_2/gold nanofilm was estimated by using the amperometric I–T technique. Upon addition of glucose to the electrolyte, the GOx could oxidize the glucose to gluconic acid and hydrogen peroxide. The electrochemical mechanism of glucose oxidation may be depicted as follows:

$$\text{glucose} + \text{GOx} \rightarrow \text{gluconic acid} + \text{hydrogen peroxide} \quad (1)$$

$$\text{hydrogen peroxide} \rightarrow 2e^- + O_2 + 2H^+ \quad (2)$$

During amperometric I–T measurements, an initial potential of −1.0 V, a sampling interval of 0.1 s, and a sensitivity of 5×10^{-6} (A/V) were applied as parameters. During the electrochemical investigation, we performed the experiments using the gold-coated silicon electrode with about 50 mm^2 area (The vertical length: 10 mm and the horizontal length: 5 mm), and using the gold-deposited polymer electrode and the gold/MoS_2/gold nanofilm on the polymer electrode with about 50 mm^2 area (The vertical length: 2.5 mm and the horizontal length: 20 mm) to match the active surface area of prepared electrodes.

2.6. Flexibility test of the fabricated biosensor

The flexibility of the fabricated biosensor was tested using a micro-fatigue tester machine. As shown in Fig. S6a, the electrode was fastened to the machine. The tip located on the upper side was then lowered to apply force to the electrode. By applying force at the center of the electrode, the electrode was bent to insert it into the gap on the bottom fixture. The flexibility of the electrode could be estimated by measuring the flexure extension due to the force applied. Therefore, rigid silicon electrodes could break since the electrode would not be able to achieve high flexure extension. The flexibility of the fabricated biosensor was investigated and compared with that of a conventional silicon electrode.

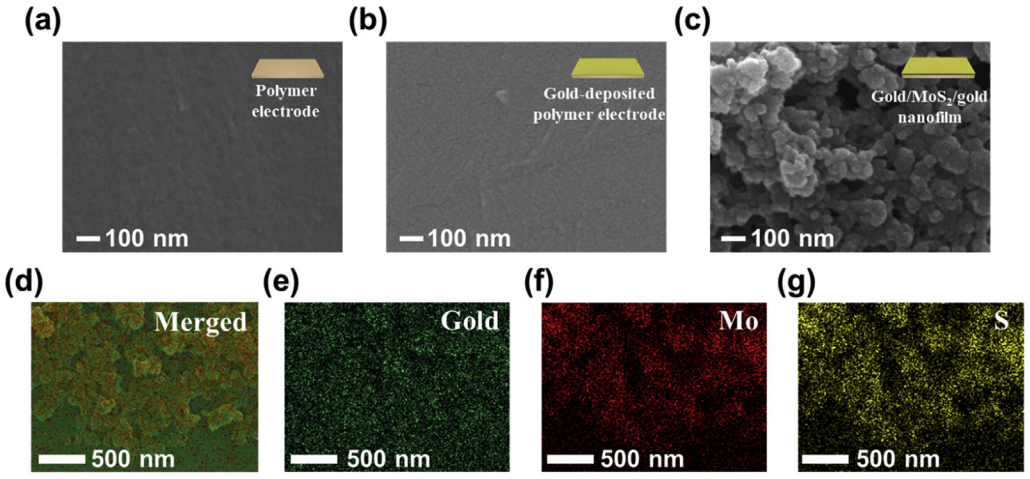

Fig. 2. SEM images of (a) the polymer electrode, (b) the gold-coated polymer electrode, and (c) the gold/MoS_2/gold nanofilm on the polymer electrode. EDS mapping results for the gold/MoS_2/gold nanofilm on the polymer electrode: (d) merged image, (e) gold, (f) Mo, and (g) S.

3. Results and discussion

3.1. Verification of the gold/MoS_2/gold nanofilm formation

SEM results for the bare polymer electrode, the gold-coated polymer electrode, and the gold/MoS_2/gold nanofilm on the polymer electrode are shown in Fig. 2. Fig. 2a shows regular grains on the surface of the bare polymer electrode. The surface of the gold-deposited polymer electrode (Fig. 2b) had small grains patterned regularly by the gold sputtered on the surface of the polymer electrode. The gold/MoS_2/gold nanofilm (Fig. 2c) showed the spin-coated MoS_2 NPs covered with gold. The size range of the spin-coated MoS_2 NPs was about 100 nm–20 nm. EDS analysis of all acquired SEM images are shown in Fig. S1. Carbon (C), nitrogen (N), and oxygen (O) in the EDS results were detected in the polymer electrode. The gold-coated polymer electrode contained C, N, O, and additional gold due to gold sputtering. EDS analysis of the gold/MoS_2/gold nanofilm showed additional molybdenum (Mo) and sulfur (S) at 1:2 ratio, which verified the existence of spin-coated MoS_2 NPs. The amount of gold was twice that in the gold-deposited polymer electrode because of the second gold layer on the spin-coated MoS_2 layer. In addition, to verify the fabrication steps of the gold/MoS_2/gold nanofilm on the polymer electrode in detail, EDS mapping results of the polymer electrode and the gold-deposited polymer electrode were compared, as shown in Fig. S2. From EDS mapping results, the gold deposition on the polymer electrode was verified due to the existence of gold element on the electrode, and Pt was derived from the metal coating for EDS sample preparation. Fig. 2d and g shows the EDS mapping images of the prepared electrode. Gold was all over the surface, as shown in Fig. 2e. The elements Mo and S existed on the location of the spin-coated MoS_2 NPs (Fig. 2f and g). The EDS mapping analysis of the other location is provided in Fig. S3. SEM and EDS analysis verified the fabrication of the gold/MoS_2/gold nanofilm on the polymer electrode.

3.2. Surface morphology of the gold/MoS_2/gold nanofilm

Fig. 3 displays the morphological results for the polymer electrode, the gold-deposited polymer electrode, and the gold/MoS_2/gold nanofilm on the polymer electrode obtained by AFM. The following parameters for AFM operation were applied: scan size of 500 nm, scan rate of 0.999 Hz, aspect ratio of 1:1, integral gain of 0.2, proportional gain of 0.4, and amplitude set point of 0.252 V. Fig. 3a shows the AFM results for the polymer electrode. The surface morphology of the polymer electrode was almost flat, with some grains similar to those in the SEM analysis. The gold-deposited polymer electrode shown in Fig. 3b had some small grains with lower height, similar to the grains detected by SEM. However, because of the limited resolution of AFM, the size of the grains seemed bigger than the grains obtained from SEM. The surface morphology of the gold/MoS_2/gold nanofilm showed the apparent shape of nanoparticles with diameters around tens of nanometers, similar to results seen in the SEM images. Vertical investigation was performed using AFM (Fig. S4). According to the vertical results, the height of the polymer electrode was around 0.8 nm, that of the gold-deposited polymer electrode was 3.6 nm, and that of the gold/MoS_2/gold nanofilm was 13.2 nm. These show the apparent height difference

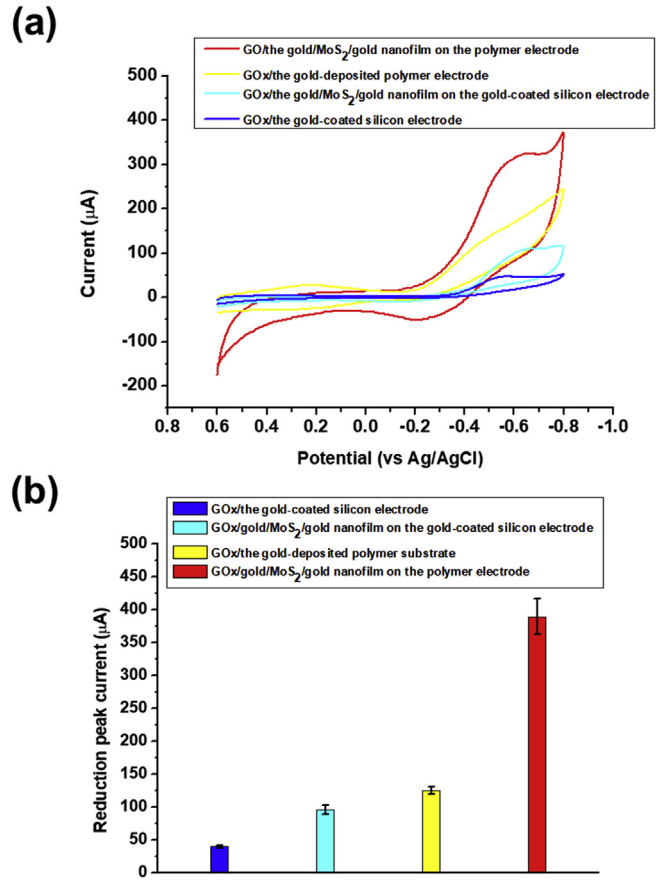

Fig. 4. Cyclic voltammograms of (a) GOx on the gold-coated silicon electrode, GOx on the gold/MoS_2/gold nanofilm on the gold-coated silicon electrode, GOx on the gold-coated polymer electrode, and GOx/gold/MoS_2/gold nanofilm on the polymer electrode. (b) Reduction peak currents of GOx on the gold-coated silicon electrode, GOx on the gold/MoS_2/gold nanofilm on the gold-coated silicon electrode, GOx on the gold-deposited polymer electrode, and GOx/gold/MoS_2/gold nanofilm on the polymer electrode. Error bars indicate the standard deviations of five different measurements.

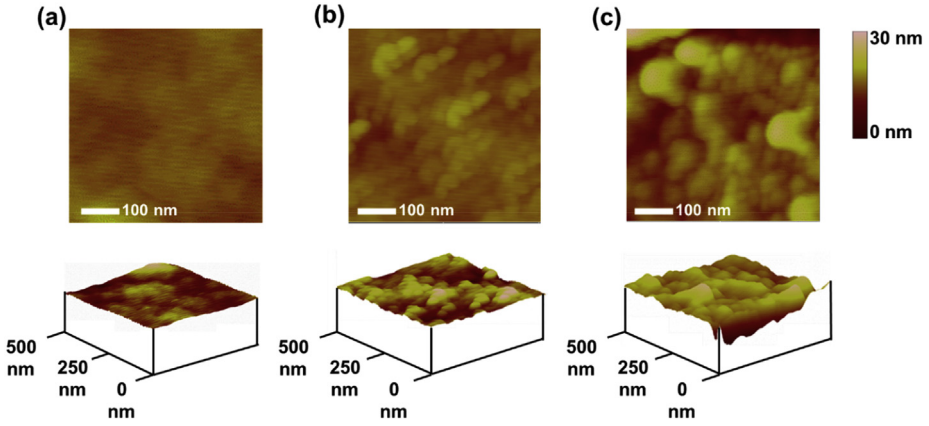

Fig. 3. AFM images of (a) the polymer electrode, (b) the gold-deposited polymer electrode, and (c) the gold/MoS_2/gold nanofilm on the polymer electrode.

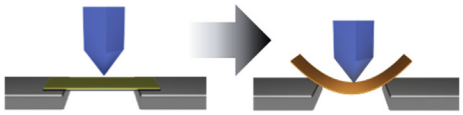

	Flexure Extension (mm)	Flexure Strength (MPa)
Conventional electrode	0.0938	307.4
Gold-deposited polymer	3.36	13.9
Gold/MoS_2/gold nanofilm	3.48	11.2

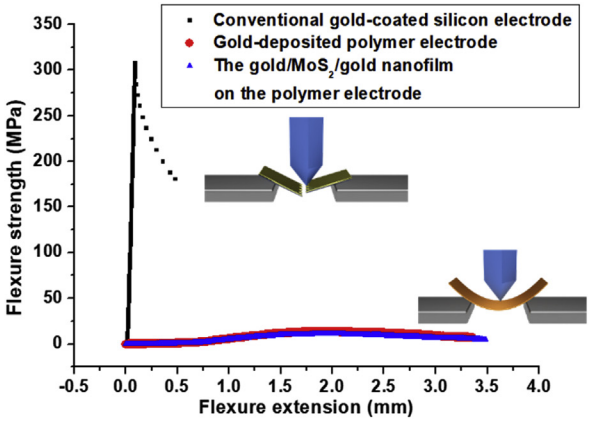

Fig. 5. Flexibility test of the gold/MoS_2/gold nanofilm on the polymer electrode.

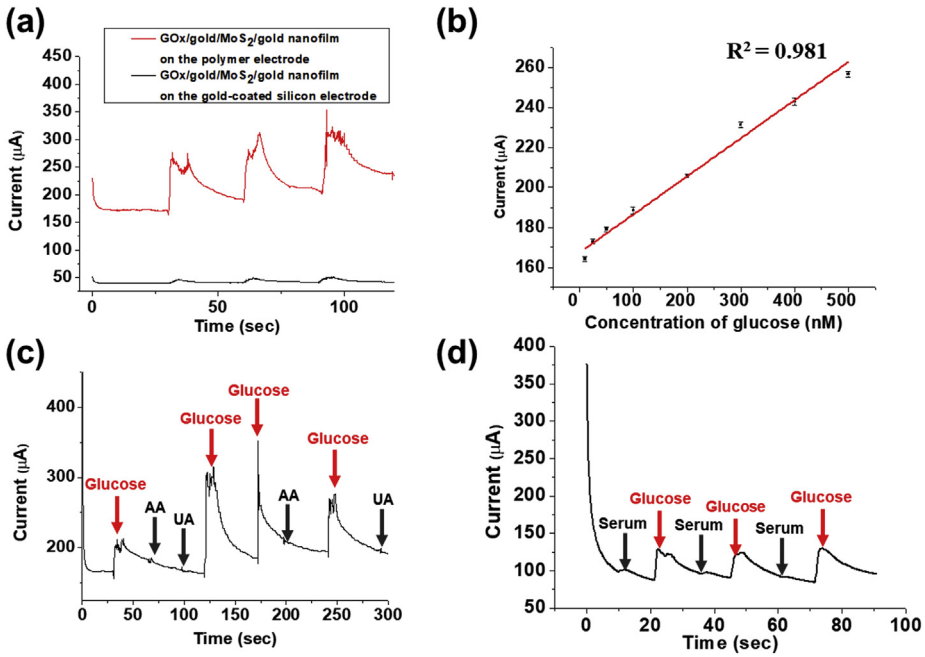

Fig. 6. (a) Amperometric responses of the GOx/gold/MoS_2/gold nanofilm on the polymer electrode and the GOx/gold/MoS_2/gold nanofilm on the gold-coated silicon electrode upon addition of 100 nM glucose. (b) Linear response graph of the GOx/gold/MoS_2/gold nanofilm on the polymer electrode upon addition of glucose from 500 nM to 10 nM. (c) Selectivity test of the GOx/gold/MoS_2/gold nanofilm on the polymer electrode upon addition of glucose with AA and UA and (d) amperometric response upon addition of 100 nM glucose to human serum and human serum without glucose.

of the control electrodes. Using the AFM and vertical investigation, we investigated the surface morphology of the gold/MoS_2/gold nanofilm on the polymer electrode.

3.3. Electrochemical properties of the fabricated biosensor

Immobilization of GOx on the gold/MoS_2/gold nanofilm was verified by the detection of the derived redox peaks due to GOx immobilization on the gold/MoS_2/gold nanofilm using CV. The electrochemical signal increment due to the gold/MoS_2/gold nanofilm was confirmed by CV using metalloprotein (Mb) and compared with the redox peaks of Mb on the gold-deposited polymer electrode (Fig. S5) to confirm the general application with other biomolecules. Fig. 4a shows the cyclic voltammograms of GOx on the gold-coated silicon electrode, GOx on the gold/MoS_2/gold nanofilm on the gold-coated silicon electrode, GOx on the gold-coated polymer electrode, and GOx/gold/MoS_2/gold nanofilm on the polymer electrode. GOx on the gold-coated polymer electrode then showed an electrochemical signal higher than that of the GOx on the conventionally used gold-coated silicon electrode. GOx on the gold-coated polymer electrode caused a 137.0 μA reduction of the peak current at around −500 mV, which was much higher than the reduction peak current (47.0 μA) of the GOx on the gold-coated silicon electrode. This result indicates that the capacitance effect of the polymer induced the increment of the overall spacing gap between the reduction line (upper line) and the oxidation line (below line), and the deposited gold on the polymer electrode induced the increment of the redox peak currents. This shows that the gold-coated polymer electrode was more suitable for electrochemical investigation as compared with the gold-coated silicon electrode. Furthermore, redox peaks of the GOx/gold/MoS_2/gold nanofilm on the polymer electrode showed a higher signal compared with those of GOx on the gold-deposited polymer electrode and GOx on the gold/MoS_2/gold nanofilm on the gold-coated silicon electrode. The reduction peak current of the GOx/gold/MoS_2/gold nanofilm on the polymer electrode was 323.0 μA, which was much higher than that of the reduction peak current values of GOx on gold-coated polymer electrode (137.0 μA) and GOx on gold/MoS_2/gold nanofilm on the gold-coated silicon electrode (106.0 μA). The reproducibility of redox peaks of the GOx/gold/MoS_2/gold nanofilm on the polymer electrode was confirmed by CV using various prepared samples. As shown in Fig. 4b, the average reduction peak current of the GOx/gold/MoS_2/gold nanofilm was 389.9 μA from five different measurements. This result indicates the apparent increase in the electrochemical signal as compared with the average reduction peak currents of GOx on the gold-coated polymer electrode (125.8 μA), GOx on the gold/MoS_2/gold nanofilm on the gold-coated silicon electrode (96.4 μA), and GOx on the gold-coated silicon electrode (39.7 μA).

3.4. Flexibility of the prepared biosensor

The flexibility test on the gold/MoS_2/gold nanofilm was done using a fatigue-test machine. Fig. 5 shows the flexibility results for the conventional gold-coated silicon electrode, the gold-coated polymer electrode, and the gold/MoS_2/gold nanofilm on the polymer electrode. The graph shows the flexure strength values for the flexure extension values of the gold-coated silicon, gold-coated polymer, and the gold/MoS_2/gold nanofilm on the polymer electrode. The flexure extension value of the conventional gold-coated silicon electrode was only 0.0938 mm upon application of a 307.4 MPa force. However, the flexure extension values for the gold-deposited polymer and the gold/MoS_2/gold nanofilm on the polymer electrode were 3.36 mm and 3.48 mm, respectively, upon application of around 12 MPa force, higher than that the for this rigid electrode. Even though the same initial force was applied to the three electrodes on the machine, the higher force was applied to the gold-coated silicon electrode because of the high rigidity of the silicon. On the other hand, only a small amount of initial force was actually applied to the gold-coated polymer and the gold/MoS_2/gold nanofilm on the polymer electrode by bending these electrodes into gaps with high flexure extension values because of the flexibility of these electrodes. The gold/MoS_2/gold nanofilm showed that the excellent flexibility derived from the polymer could be utilized as an appropriate platform for the development of a wearable biosensing system. After the gold/MoS_2/gold nanofilm on the polymer electrode was bent, the electrode after bending was investigated by CV to estimate the influence of the bending on the electrochemical performance of the prepared flexible biosensor. According to the electrochemical results, the bending did not affect the electrochemical performance of this flexible biosensor, as shown in Fig. S6b, which shows the averaged reduction peak current after bending (383.7 μA) from five different measurements. This was comparable to 389.9 μA for the GOx/gold/MoS_2/gold nanofilm on the polymer electrode before bending. In addition, the GOx/gold/MoS_2/gold nanofilm on the polymer electrode after bending was observed by EDS mapping analysis to verify the stable immobilization of the gold/MoS_2/gold nanofilm on the polymer electrode (Fig. S6c). This result shows that the gold/MoS_2/gold nanofilm on the polymer electrode retained its components after bending similar to the EDS mapping results of the gold/MoS_2/gold nanofilm on the polymer electrode before bending (Fig. 2) because bending did not hugely affect the nanoscale layers.

3.5. Amperometric response of the fabricated biosensor by glucose addition

The glucose-sensing experiment using the amperometric I–T technique was conducted to estimate the glucose-sensing performance of the fabricated biosensor. The conventional three-electrode system was applied to perform glucose sensing. The amperometric-response curve of the biosensor was obtained by addition of 10 μL of 10 mM glucose (100 nM) in 5 mL of the PBS solution to the biosensor. Fig. 6 shows the amperometric response curve of the GOx/gold/MoS_2/gold nanofilm upon addition of glucose (Fig. 6a), which increased steeply and reached a stable state with uniform increments. Furthermore, it shows the apparent increase in amperometric response relative to GOx on the gold/MoS_2/gold nanofilm on the gold-coated silicon electrode similar to the results in CV analysis. Fig. 6b shows the linear response graph of the biosensor upon addition of glucose from 500 nM to 10 nM. This biosensor had a detection limit of 10 nM. Table S1 shows a comparison of detection limits for biosensors. To verify the selectivity of the biosensor, AA and UA with glucose were added. The fabricated biosensor displayed an appreciable amperometric response (Fig. 6c) as compared with the others and only a small noise current upon the addition of glucose. To verify the sensing of glucose by this biosensor in an actual sample, the glucose prepared in human serum (100 nM amounts) was added (Fig. 6d). According to the amperometric response, this biosensor could detect only glucose in the human serum, and it did not show any amperometric responses when it was added to the serum without glucose.

4. Conclusions

In this study, a flexible electrochemical biosensor composed of GOx/gold/MoS_2/gold nanofilm on a polymer electrode was developed for the first time to detect glucose with electrochemical signal enhancement and flexibility. To achieve this, sputter deposition of gold and spin coating of MoS_2 were performed as part of a simple fabrication process. The fabricated biosensor showed an increased electrochemical signal, with a 389.9 μA average reduction peak current as compared with the result of the GOx on the gold-deposited polymer electrode (125.8 μA). This biosensor also showed an increased amperometric glucose-sensing performance with 10 nM detection limit, which suggested more sensitivity than that of previously reported flexible glucose sensor, and could detect glucose dissolved in the human serum. Due to the flexible polymer electrode used as substrate, this biosensor showed flexibility greater than that of the rigid sensor using a conventional gold-coated silicon electrode (0.09 mm), with a flexure extension of 3.48 nm. However, optimization of layer depth should be required in the future work to apply for practical wearable biosensors. In conclusion, the proposed flexible glucose biosensor composed of an enzyme/gold/MoS_2/gold nanofilm on the polymer electrode can be utilized as a flexible sensing platform to develop a wearable biosensing system in the future.

Declaration of interests

The authors declare that they have no known competing financial interests or personal relationships that could have appeared to influence the work reported in this paper.

CRediT authorship contribution statement

Jinho Yoon: Conceptualization, Investigation, Formal analysis, Writing - original draft, Writing - review & editing. **Sang Nam Lee:** Investigation, Funding acquisition, Writing - review & editing. **Min Kyu Shin:** Investigation, Validation. **Hyun-Woong Kim:** Formal analysis, Writing - original draft. **Hye Kyu Choi:** Formal analysis, Validation. **Taek Lee:** Validation, Writing - original draft. **Jeong-Woo Choi:** Conceptualization, Project administration, Supervision, Writing - original draft, Writing - review & editing.

Acknowledgment

This research was supported by Scien US Inc.

Appendix A. Supplementary data

Supplementary data to this article can be found online at https://doi.org/10.1016/j.bios.2019.111343.

References

Abikshyeet, P., Ramesh, V., Oza, N., 2012. Diabetes Metab. Syndr. Obes. 5, 149–154.
Acerce, M., Akdogan, E.K., Chhowalla, M., 2017. Nature 549, 370.
Ahammad, A.J.S., Mamun, A.A., Akter, T., Mamun, M.A., Faraezi, S., Monira, F.Z., 2016. J. Solid State Electrochem. 20, 1933–1939.
Alberti, K.G.M.M., Zimmet, P.Z., 1998. Diabet. Med. 15, 539–553.
Baghayeri, M., Amiri, A., Farhadi, S., 2016. Sens. Actuators B-Chem. 225, 354–362.
Chaichi, M.J., Ehsani, M., 2016. Sensor. Actuator. B Chem. 223, 713–722.
Fenzl, C., Hirsch, T., Baeumner, A.J., 2016. Trac. Trends Anal. Chem. 79, 306–316.
Ferri, S., Kojima, K., Sode, K., 2011. J. Diabetes Sci. Technol. 5, 1068–1076.
Gardin, C., Piattelli, A., Zavan, B., 2016. Trends Biotechnol. 34, 435–437.
Kang, H., Jung, S., Jeong, S., Kim, G., Lee, K., 2015. Nat. Commun. 6, 6503.
Lee, T., Kim, S.-U., Min, J., Choi, J.-W., 2010. Adv. Mater. 22, 510–514.
Lee, T., Lee, Y., Park, S.Y., Hong, K., Kim, Y., Park, C., Chung, Y.-H., Lee, M.-H., Min, J., 2019a. Colloid Surf. B-Biointerfaces 175, 343–350.

Lee, T., Park, S.Y., Jang, H., Kim, G.H., Lee, Y., Park, C., Mohammadniaei, M., Lee, M.-H., Min, J., 2019b. Mater. Sci. Eng. C 99, 511–519.
Manson, J.A., Colditz, G.A., Stampfer, M.J., 1991. Arch. Intern. Med. 151, 1141–1147.
Min, J., Lee, T., Oh, S.–M., Kim, H., Choi, J.-W., 2010. Biotechnol. Bioproc. Eng. 15, 30–39.
Mohammadniaei, M., Yoon, J., Lee, T., Bapurao, B., Lee, D., Choi, J.-W., 2018. Small 14, 1703970.
Ray, K.K., Seshasai, S.R.K., Wijesuriya, S., Sivakumaran, R., Nethercott, S., Preiss, D., Erqou, S., Sattar, N., 2009. The Lancet 373, 1765–1772.
Reimhult, K., Yoshimatsu, K., Risveden, K., Chen, S., Ye, L., Krozer, A., 2008. Biosens. Bioelectron. 23, 1908–1914.
Rogers, K.R., 2006. Anal. Chim. Acta 568, 222–231.
Schuhmann, W., Ohara, T.J., Schmidt, H.L., Heller, A., 1991. J. Am. Chem. Soc. 113, 1394–1397.
Shafiee, H., Asghar, W., Inci, F., Yuksekkaya, M., Jahangir, M., Zhang, M.H., Durmus, N.G., Gurkan, U.A., Kuritzkes, D.R., Demirci, U., 2015. Sci. Rep. 5, 8719.
Torimoto, K., Okada, Y., Mori, H., Tanaka, Y., 2013. Cardiovasc. Diabetol. 12, 1.
Tuomilehto, J., Lindström, J., Eriksson, J.G., Valle, T.T., Hämäläinen, H., Ilanne-Parikka, P., Keinänen-Kiukaanniemi, S., Laakso, M., Louheranta, A., Rastas, M., Salminen, V., Aunola, S., 2001. N. Engl. J. Med. 344, 1343–1350.
Tyona, M.D., 2013. Adv. Mater. Res. 2, 195–208.
Wang, H., Lu, Z., Xu, S., Kong, D., Cha, J.J., Zheng, G., Hsu, P.-C., Yan, K., Bradshaw, D., Prinz, F.B., Cui, Y., 2013. Proc. Natl. Acad. Sci. Unit. States Am. 110, 19701–19706.
Wang, J., Wu, Z., Hu, K., Chen, X., Yin, H., 2015. J. Alloy. Comp. 619, 38–43.
Wang, L., Jackman, J.A., Ng, W.B., Cho, N.-J., 2016a. Adv. Funct. Mater. 26, 8623–8630.
Wang, S., Chinnasamy, T., Lifson, M.A., Inci, F., Demirci, U., 2016b. Trends Biotechnol. 34, 909–921.
Wilson, R., Turner, A.P.F., 1992. Biosens. Bioelectron. 7, 165–185.
Wu, C., Sun, H., Li, Y., Liu, X., Du, X., Wang, X., Xu, P., 2015. Biosens. Bioelectron. 66, 350–355.
Yang, Y., Yang, X., Zou, X., Wu, S., Wan, D., Cao, A., Liao, L., Yuan, Q., Duan, X., 2017. Adv. Funct. Mater. 27, 1604096.
Yoo, E.H., Lee, S.Y., 2010. Sensors 10, 4558–4576.
Yoon, J., Lee, T., Bapurao, B., Jo, J., Oh, B.-K., Choi, J.-W., 2017a. Biosens. Bioelectron. 93, 14–20.
Yoon, J., Shin, J.-W., Lim, J., Mohammadniaei, M., Bapurao, B., Lee, T., Choi, J.-W., 2017b. Colloid Surf. B-Biointerfaces 159, 729–736.
Zhao, W.-W., Xu, J.-J., Chen, H.-Y., 2017. Biosens. Bioelectron. 92, 294–304.
Zhao, P., Tang, Q., Zhao, X., Tong, Y., Liu, Y., 2018. J. Colloid Interface Sci. 520, 58–63.
Zhu, Z., 2017. Nano-Micro Lett. 9, 25.